Insights into Structure and Elastic Thickness of Ridge Belts on Venus. Zachary W. Williams[1], Paul K. Byrne[1], and Jeffrey A. Balcerski[2]. [1]Planetary Research Group, Department of Marine, Earth, and Atmospheric Sciences, North Carolina State University, Raleigh, NC 27695 (zwwillia@ncsu.edu), [2]Ohio Aerospace Institute, Cleveland, OH 44142.

Introduction: Despite Venus showing no evidence of a global system of tectonic deformation, a variety of tectonic landforms across Venus suggests a complex and active geologic history that is not fully understood. Widely distributed within Venus' low-lying plains are linear to arcuate, positive-relief systems of shortening structures, termed ridge belts in the literature[1–7]. Although these landforms have been recognized for some time, the relatively recent availability of regional topographic data at resolutions greater than the Magellan altimetry dataset [8] allows the morphology and structure of ridge belts to be studied in finer detail.

Here, our aim was to acquire detailed morphometric data for a globally distributed set of ridge belts. Once such data were acquired, we mapped observable tectonic structures—faults and folds—within a subset of those selected ridge belts. We then used topographic profiles and relief values from the collected morphometric data to acquire local estimates for the effective elastic thickness of the lithosphere, evidenced by flexural signatures in topography proximal to these ridge belts.

Data and Methods: We utilized global Magellan synthetic aperture radar (SAR) full-resolution radar map (FMAP) 75-meter-per-pixel (m/px) left- and right-look mosaics for the initial identification of candidate ridge belts. For topographic measurements, we used stereo-derived digital elevation models (DEMs) produced by Herrick et al. [8], which offer ~20% global coverage at 1–3 km/px resolution.

Morphological analysis: We conducted a global survey with ArcGIS to identify ridge belts on the basis of morphological descriptions from existing studies [e.g., 1, 4–7, 9]. Our survey yielded 24 candidates for further analysis that have a well preserved morphology and are not obviously kinematically associated with neighboring systems. Of these 24 structures, 12 are within the Herrick DEM coverage [8]. We recorded the strike of each landform and width measurements (representing the distance across strike to opposing boundaries of the landform) at regular intervals along the structure. For those ridges covered by the Herrick DEMs, we extracted 20 cross-sectional profiles at the point of width measurements. Relief values were extracted from topography data using the area of the ridge belt as a mask to extract pixel values from the DEM.

Fault Mapping: Identification and mapping of faults was conducted using the left- and right-look SAR survey global mosaics at 1:200,000 view scale for six ridge belts (with an example shown in **Fig 1a**). These six were selected on the basis of their orientation relative to the look directions of the Magellan radar, and coverage by both left- and right-look SAR data. Assuming a similar surface mineralogy across the ridge belts, the variation in backscatter (the value gathered by SAR) is a function of surface roughness and incidence angle [10]. Radar bright lineations are thus interpreted as alterations in surface angle due to faulting. On the basis of comparison with tectonic structures on Earth and other rocky bodies, we interpreted arcuate fault traces as denoting shortening structures (likely folds atop thrust faults) [11]. Linear fault traces, commonly offset in an *en echelon* manner, were taken to correspond to normal faults. The orientation of the six ridge belts orthogonal to the Magellan radar look-directions means that the survey in which a lineation is prominently displayed denotes the direction of the steeper fore-limb and therefore up-dip direction. This method was statistically supported by calculating the vector mean of each fault population and using the resultant length to quantify distribution of orientation.

Lithospheric Flexure: Cross-sectional profiles were reviewed for topographic signals associated with the flexure of the elastic lithosphere in response to the mass of the ridge belt, representing a line load, akin to a seamount chain [12]. Four of the selected ridge belts displayed evidence of lithospheric flexure as resolved by the Herrick DEM data [8] (**Fig 2)**. The solution to the topographic response to a line load (represented as a point load on a 1-dimensional profile), *w*, is given by the dampened sinusoidal function [12]:

$$w = w_0 e^{-\frac{x}{a}}\left(\cos\left(\frac{x}{a}\right) + \sin\left(\frac{x}{a}\right)\right), \quad [1]$$

where w_0 is the maximum amplitude of flexure along the breadth of the profile, *x*, with respect to the flexural parameter, *a*, given by the relation:

$$a = \sqrt[4]{\frac{4D}{(\rho_m - \rho_i)g}}, \quad [2]$$

where *D* is the flexural rigidity, $\rho_m - \rho_i$ is the difference between mantle and atmospheric density, and g is the acceleration due to gravity. Flexural rigidity is given by

$$D = \frac{E}{12(1-\nu^2)}h^3, \quad [3]$$

where *E* is Young's modulus, ν is Poisson's ratio, and *h* is the depth of the elastic lithosphere. Values for Young's modulus and Poisson's ratio for anhydrous basalt, and density contrast across the lithosphere, were taken from previous studies of lithospheric flexure on Venus [13, 14]. The depth of the elastic lithosphere was determined using a least-squares optimization of a cost function for the set of equations using a simplex method, with *h* and w_0 as two of the free parameters.

Results and Discussion: The average width of the 24 ridge belts we selected is 81 km (with a maximum width value of 207 km, a minimum width of 9 km). The standard deviation of width measurements within each ridge belt ranged from 59 to 4 km, with an average value of 19 km. For the 12 ridges within the DEM coverage, we found an average relief value of 597 m and a median value of 551 m (with maximum and minimum values of 938 m and 232 m, respectively). The uniform low relief values, not exceeding 1 km despite width values of

9 to 207 km, are thus the most consistent morphological parameter. Cross-sectional profiles of the ridge belts commonly display an observable fore- and back-limb morphology consistent with thrust-fault-related landforms.

Fault Analysis: Mapping and morphological assessment indicate that tectonic structures within ridge belts are predominately thrust faults and their related folds (**Fig 1b)**, the majority of which strike roughly parallel with the long axis of the host ridge belt (**Fig 1c**). The cumulative lengths of fault populations, discretized by dip-direction, were compared within a given ridge belt to determine if a dominant fault dip direction is present within that belt. This analysis yielded a direction of tectonic transport that agrees with that suggested by the fore- and back-limb morphology seen in cross-sectional profiles for ridge belts that displayed this asymmetry. Thrusts within the ridge belts commonly form antithetic thrust pairs and imbricated anticlines (**Fig 1b**), the distance between which may offer information regarding homogeneity in slip and fault dip angle along major underlying fault planes [15]. The spacing distribution of surface anticlines varies among the ridge belts we included (**Fig 1d**). We interpret this spatial variation to reflect heterogeneities in the properties of the major faults comprising these ridge belts. Our interpretation leads to the view that ridge belts are complex systems of thrust fault duplexes, in contrast to shortening structures on other worlds that are often morphologically more simple.

Lithospheric Flexure: Results for depth of the elastic lithosphere supporting each ridge return values of 10–24 km (**Fig 2**), largely consistent with previous studies for the planet's lowlands [e.g., 16–18]. The optimization function was run with an unbounded number of iterations, and solutions represent a best fit of modelled solutions to the observed curvature of the foreland basin flanking the ridge belts (**Fig 2**). The range of values given by these model results, along with the low-relief values we measured, support the hypothesis that the elastic lithosphere surrounding these ridge belts is relatively thin, compared to the breadth and length values of these landforms and to the crusts of other terrestrial planets. Furthermore, this result agrees with predictions of yield strength envelopes that suggest a thin elastic lithosphere as a function of Venus' high surface temperature [19]. This inference can be further tested with forward modeling of ridge belt morphology [20].

References: [1] Frank, S. L. and Head, J. W. III. (1990) *Earth, Moon, and Planets.* [2] Ivanov, M. A. and Head, J. W (2013) *Planetary and Space Science, 84.* [3] Barsukov, V. L. et al. (1986) *JGR, 91.* [4] McGill, G. E. and Campbell, B. A. (2006) *JGR, 111.* [5] Ivanov, M. A. and Head, J. W. (2011) *Planetary and Space Science, 59.* [6] Solomon, S. C. et al. (1992) *JGR, 97.* [7] Basilevsky, A. T. and Head, J. W. (2003) *Report on Progress in Physics, 66.* [8] Herrick, R. R. et al. (2012) *EOS, 93, No. 12.* [9] Balcerski, J. A. and Byrne, P. K. (2018) *LPSC 2018,* abstract 2083. [10] Farr, T. G. (1993) *Guide to Magellan Image Interpretation.* [11] Burg, JP. (2017) *Tectonics: Thrust Systems.* [12] Lowrie, W. (2007) *Fundamentals of Geophysics.* [13] O'Rourke, J. G. and Smrekar, S. E. (2018) *JGR, 123.* [14] Schultz, R.A (1993) *JGR, 98.* [15] Anderson, F. S. and Smrekar, S. E. (2006) *JGR, 111.* [15] James, P.B. et al. (2012) *JGR, 118.*[16] Buck, W.R. (1992) *Geophysical Research Letters, 19.* [17] Ghail, R. (2015) *Planetary and Space Science, 113-114.* [18] Balcerski, J. A. and Byrne, P. K. (2018) *VEXAG 2018,* abstract 2137.

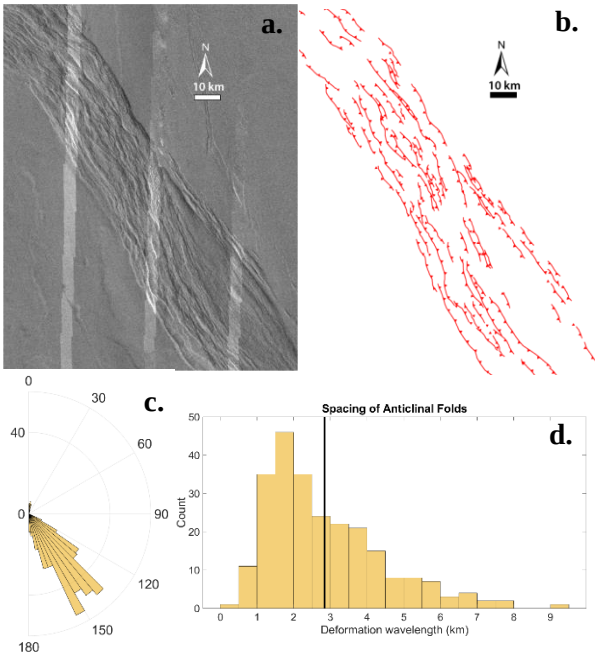

Fig. 1a. An example ridge belt centered at 41.2° S, 20.7° E. in overlain left- and right-look SAR at 1:200,000 view scale. **b.** Mapped thrust fault traces interpreted from the SAR. Teeth indicate the dip direction of the faults **c.** Distribution of anticline spacing for the example ridge belt with a mean of 2.8 km, indicated by the red line, and median of 2.1 km. The is no evidence of spatial relationships. **d.** Thrust faults are striking with a vector mean of 143.7° with a resultant length of 0.891. This value indicates minimal variation and represents a single fault population

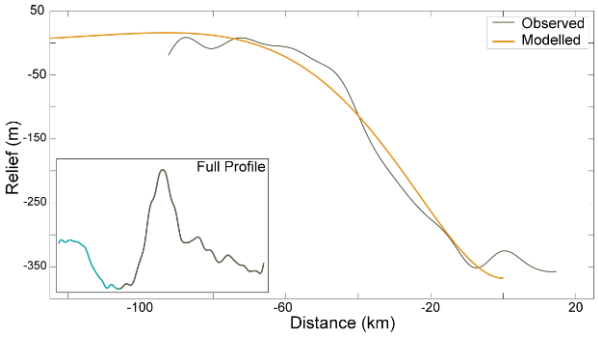

Fig. 2. Example of least-squares optimized fit to the observed topographic response of the lithosphere to the mass-loading of a ridge belt centered at 5.6 S, 162.2 E Results from this model indicate a lithospheric thickness of 10.4 km